CCITT SGXV
Working Party XV/1
Experts Group for ATM Video Coding

Document AVC-267
July 1-10 1992

Source : RTT BELGACOM

Title : Bit rate statistics of a TV distribution codec

Purpose : Information

---

1. Introduction

A hardware prototype of a TV distribution codec has been developed in the frame of the Belgian Broadband Experiment (BBE).

Meanwhile, the prototype codec has been used to gather realistic statistics of the output bit rate for TV distribution in the VBR mode. For this purpose about 2 hours of the TV programme transmitted by a Belgian Broadcasting Organization (RTBF) have been recorded in the studio using a D1 machine. The prototype codec was operated on this material for various values of the transmission factor (i.e. of the basic picture quality) and a data base of cell rate and of inter-arrival times has been collected. The aim of this document is to present some statistical results obtained by processing the database.

2. Experimental conditions

The BBE codec is a hybrid DCT codec. Main differences with the CCIR Rec. 723 codec are listed below. The loop operates 8×8 DCT blocks taken in a pseudo-progressive format obtained by merging the odd and even fields. It does not include motion compensation.

The quantizing law is roughly similar to the one defined in CCIR Rec. 723, in the sense that the quantizer step is calculated in function of the same parameters, i.e. Y/C, coefficient order, block criticality and transmission factor. In the VBR mode the transmission factor is maintained constant instead of being controlled by the level of buffer occupancy. Only in emergency conditions, i.e. for avoiding to violate the contract negotiated with the network, the transmission factor will be momentarily increased. This fall-back mode was not activated in the experiment described here, i.e. no policing function was activated.

The VLC used in the BBE codec is the U-VLC developed in the frame of this programme. The video framing structure is quite similar to that of the Rec. 723 codec. There is some difference with the latter however, because the U-VLC (based on the frequency scanning principle) processes sequences of DCT coefficients with the same order taken along a slice, starting with the low-order coefficients. As a result, the instantaneous bit rate is decreasing during a slice. In the rec. 723 codec on the contrary, the VLC operates on DCT blocks and the output bit rate during a slice is

more or less constant.

The output bit stream of the video framing feeds a packetizer which forms cells according to the CCITT recommendations. In the experiment which was carried out, once the video framing has delivered enough bits to fill a cell, this cell is launched in the network "as soon as possible". This mechanism is not necessarily representative of what should be done in practice, but it is the best suited to gathering information.

For clarity it is useful to say explicitely what means "as soon as possible" in the previous paragraph. The ATM links operate at the bit rate of 150 Mbit/s. Cells contain 53 bytes. This means that the bit rate along the ATM links is clocked in time slots at the cell rate or *cell frequency* given by

$$f_c = \frac{150 \times 10^6}{53 \times 8} = 353773 \quad Hz \tag{1}$$

"as soon as possible" means that when a cell is ready, it is inserted in the following time slot.

Thus the buffering mechanism used in the packetizer is kept to the strict minimum imposed by the need to wait for enough bits to fill a cell and by the timing of the ATM links. The term *bufferless packetizing* is probably adequate to describe this situation.

In the experiment which was carried, the recorded quantity was the *inter-arrival data* sequence, containing the sequence of the number of time slots between two successive emitted cells. Recording this information for a 2 hours TV programme and in addition for several values of the transmission factor would lead to a huge data base. This why this type of information was collected only for 20 minutes of the whole programme. For the remaining part of the time, the recorded quantity was the number of cells emitted per slice.

The videoframing is organized here in 76 slices made of 72 active slices and of 4 additional slices containing other information. The following reference frequencies will be used in the document: the frame frequency

$$f_f = 25 \quad Hz \tag{2}$$

and the slice frequency

$$f_s = 25 \times 76 = 1900 \quad Hz \tag{3}$$

The ratio

$$f_c/f_s \simeq 186 \tag{4}$$

is noteworthy: it indicates the number of cells/slice which would saturate a 150 Mbit link.

3. Statistics at the cell level

3.1. Statistics of inter-arrival times

The inter-arrival times $I(n)$ have been defined by the time elapsed between the generation of two consecutive cells. In the rest of the document, the inter-arrival times $I(n)$ will be discretized by

the number of slots embedded between two consecutive cells the reference for computation being the beginning of the time slot. To visualize this phenomenon, a first set of diagrams shows bars with amplitudes equal to the values of the inter-arrival times. The consecutive inter-arrival times are presented from left to right.

Different values of the transmission factor (quantization stepsize) have been considered: 5, 10, 20, 30 and 40. The correspondance between transmission factor and quality level is described below :

TxF = 05 - 10 : contribution quality
TxF = 20 - 30 : distribution quality
TxF > 35 : poor quality

The values of the first distribution moments of the inter-arrival times $I(n)$ (the mean m_I and the standard deviation σ_I expressed in inter-arrival time) are gathered in table 1 in function of the transmission factor value TxF.

Figures 1 to 5 present the inter-arrival time values on a few slices. By example, figure 1 is drawn at a transmission factor of 5 and displays about five slices. The cell generation can be thought in any case as a repetitive process with a slice period: the beginning of each slice is made of an active segment with random generations of cells followed by a silent segment without any cell generation.

Figure 1 shows groups of small inter-arrival times are followed by a longer inter-arrival time (30-45 time slots); a pattern of about twenty-five cells is replicated five times. This behaviour is due to the frequency scanning of the VLC which processes a complete slice and ends its job when all the coefficients to be transmitted are encoded.

The process is repeated at the beginning of each slice when a complete set of coefficients is ready to be encoded. When the value of the transmission factor increases, the number of cells to be launched per slice in the network decreases, the inter-arrival times in the active segment increase but, as it appears on the diagrams, the duration of the silent period remains unchanged. The whole inter-arrival time Statistics depend on both the Statistics of the sequence to be encoded and on the value of the transmission factor.

TxF	m_I	σ_I
5	6.7	11.5
10	9.9	14.8
20	13.4	17.0
30	16.9	18.7
40	19.6	19.8

Table 1: mean and standard deviation
of the inter-arrival time $I(n)$

The probability distributions of the inter-arrival times $I(n)$ are given on figures 6 to 10 for the different transmission factor values (probability of the inter-arrival time versus the discretized inter-arrival time value). It can be directly seen that they are all limited at a value around 50 time slots and that a component around 175 is present in all the diagram with a small mass of probability.

The mass at 175 corresponds to the blanking slices (four of them are present in each image, among them, one has a zero cell rate) where approximately no cell is transmitted.

The limit at 50 time slots correspond to the slowest packetization process reached when all the coefficients are equal to zero. The distribution of the inter-arrival times are quasi-exponential at high bit rates (low values of the transmission factor). When the bit rate decreases, the masses of probability spreads over the whole range of time slots [0-50].

3.2. Cell rate for unbuffered packetization

In this section, the cell rates under investigation are the instantaneous cell rates $R_U(n)$ of the codec in a bufferless packetizing scheme.

Let us begin with defining the instantaneous cell rate. The instantaneous cell rate is inversely proportional to the values of the inter-arrival process. The maximum cell rate value or the peak instantaneous cell rate is reached when one cell is delivered per time slot i.e. at the cell frequency f_c. All other cell rates are an integer fraction of this maximum. In the rest of the section, the instantaneous bit rates are normalized by the maximum value. If n slot times separate the beginning of two consecutive cells, then n samples of the instantaneous cell rate take the value $\frac{1}{n}$ on this interval.
The peak cell rate observed at the different values of the transmission factor was the maximum cell rate of one cell per time slot.. The mean and the standard deviation m_{R_U} and σ_{R_U} are gathered into table 2 with respect of different values of the transmission factor TxF.

TxF	m_{R_U}	σ_{R_U}
5	0.14	0.177
10	0.101	0.156
20	0.076	0.122
30	0.060	0.096
40	0.052	0.082

Table 2: mean and standard deviation
of the instantaneous cell rates $R_U(n)$.

To further analyze the instantaneous bit rate, the power spectrum can be considered : figures 11 to 15 present the spectrum of the instantaneous cell rate at different values of the transmission factor. The diagrams sketch the power spectrum expressed in $(\frac{cell}{cell\ \ period})^2$ versus the frequency normalized by the sampling frequency equal to the cell frequency f_c. The components at multiples of the slice frequency show up in the spectrum.

4. Statistics at the slice level : Cell rate for slice buffered packetization

In this section, the cell rate is estimated on fixed time intervals with a length of one slice. Restated in other words, the cell rates are those obtained by accumulating the cells into a buffer over periods equal to one slice. The slice cell rates $R_S(n)$ given in table 3 have been estimated over a record of 95 minutes at different values of the transmission factor TxF. Table 3 gathers the mean m_{R_S} and the standard deviation σ_{R_S} both expressed in $\frac{cell}{slice}$.

TxF	m_{R_S}	σ_{R_S}
5	25.7	10.9
10	18.1	7.2
20	13.6	5.4
30	10.7	4.5
40	9.2	3.6

Table 3: Statistics of the slice cell rate $R_S(n)$.

Figures 16 to 20 show the slice cell rates (cells per slice) with a bar graph representation in function of consecutive slice intervals at different values of the transmission factor. Each field begins with a slice with a zero cell rate. A property of the slice cell rate shows up immediately: the image periodicity with a periodicity of 76 slices (cyclo-stationary processes).

Figures 21 to 25 present the probability distributions of the slice cell rates (probability of the slice cell rate versus the cell rate). Even after 95 minutes of recording, the distributions are never really Gaussian.

5. Statistics at the frame level : bit rate for image buffered packetization

In this section, the bit rate is estimated on fixed time intervals with a length of one frame. Restated in other words, the bit rates are those obtained by accumulating the bit stream into a buffer over periods equal to one frame. The image bit rates $R_I(n)$ given in table 4 have been estimated over the same record of 95 minutes as in the previous section at different values of the transmission factor.

Table 4 gathers the mean m_{R_I} and the standard deviation σ_{R_I} both expressed in $\frac{cells}{image}$.

TxF	m_{R_I}	σ_{R_I}
5	1953	601
10	1376	321
20	1034	256
30	813	223
40	700	179

Table 4: Statistics of the image cell rates $R_I(n)$.

What is significant in this table is the relative constant value of the ratio 'standard deviation to mean' which stays around 0.26.

Figures 26 to 30 display as an example the image bit rates in function of 200 consecutive images to overview some scenes changes.

Figures 31 to 35 present the probability distributions of the image bit rates. The distribution is not really a Gaussian law.

6. Conclusions

Cell inter-arrival times and slice cell rates have been described for the BBE codec, one example of VBR codec dedicated to transmit on ATM networks. This analysis will allow to go one step further: the estimation of the multiplexing performances of VBR TV sources and the determination of the police functions to be applied on TV codecs.

References

[1.] RTT Belgium : *Video Codec developed in the Belgian Broadband Experiment*, CCITT SGXV EG ATM Video Coding, Den Haag, November 1990.

[2.] UCL : *Bit rate statistics of TV distribution codecs in the VBR mode*, COST 211ter Simulation subgroup, Hannover, May 1992.

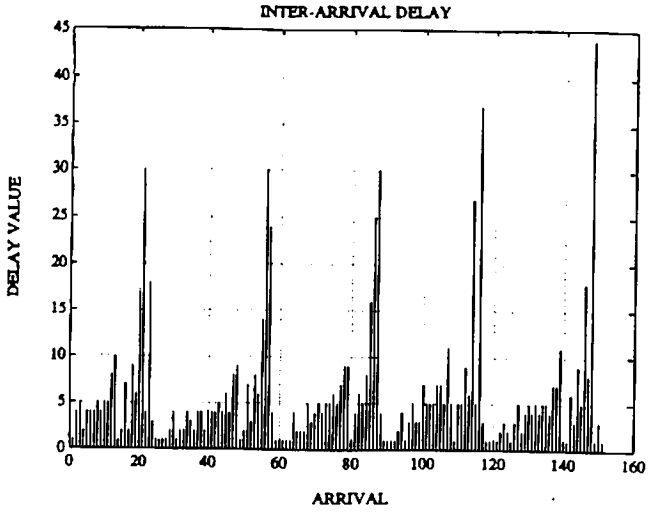

Figure 1: inter-arrival delays I(n) at TxF=5

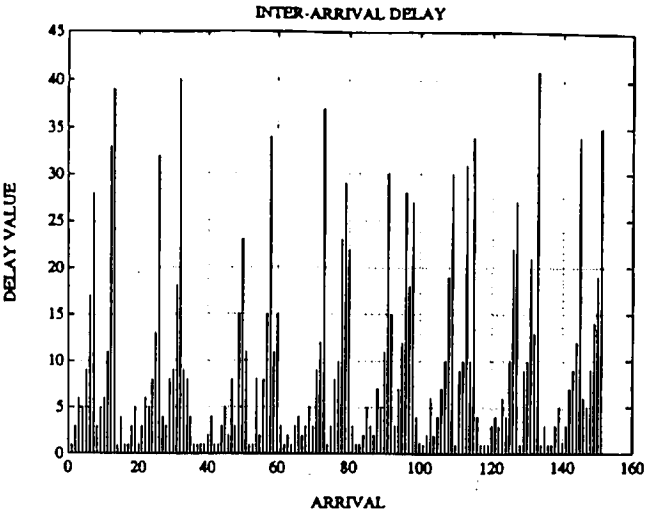

Figure 2: inter-arrival delays I(n) at TxF=10

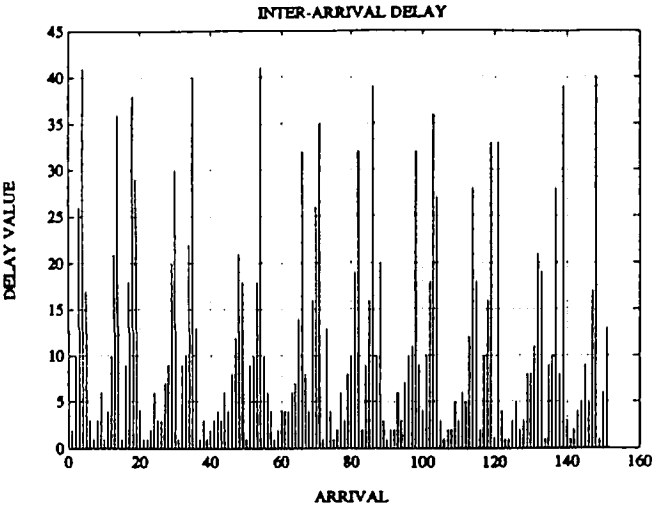

Figure 3: inter-arrival delays I(n) at TxF=20

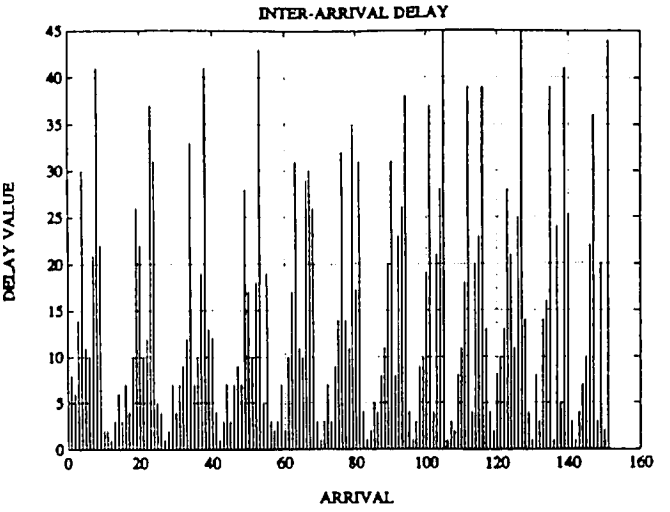

Figure 4: inter-arrival delays I(n) at TxF=30

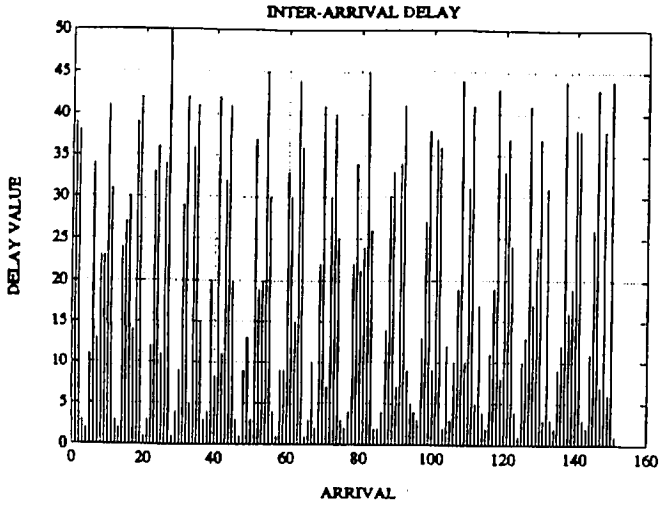

Figure 5: inter-arrival delays I(n) at TxF=40

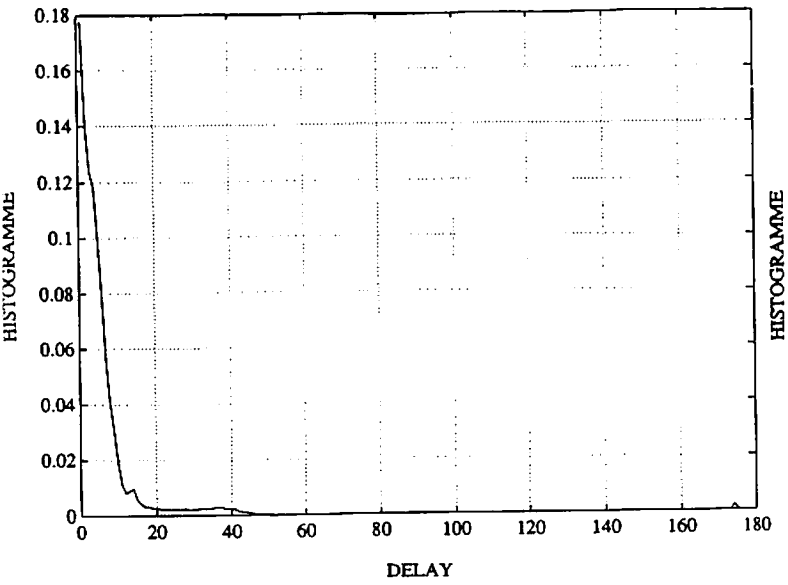

Figure 6: inter-arrival distribution at TxF=5

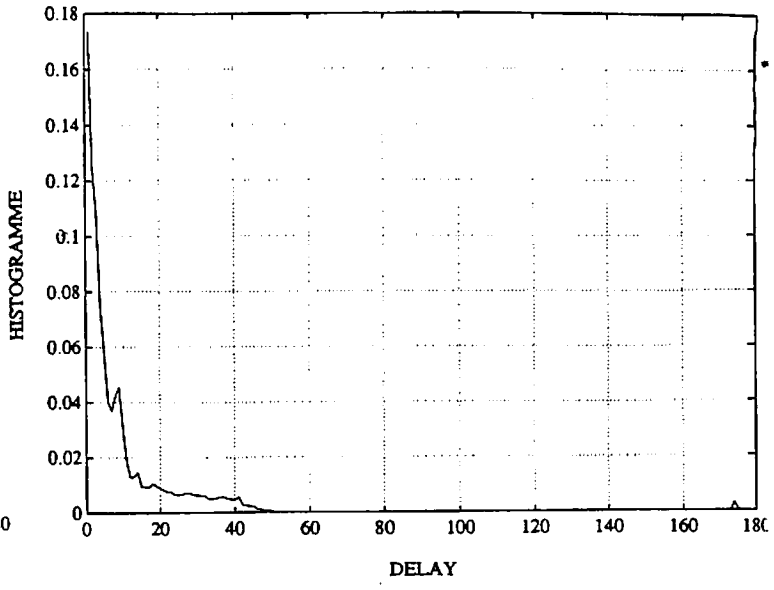

Figure 7: inter-arrival distribution at TxF=10

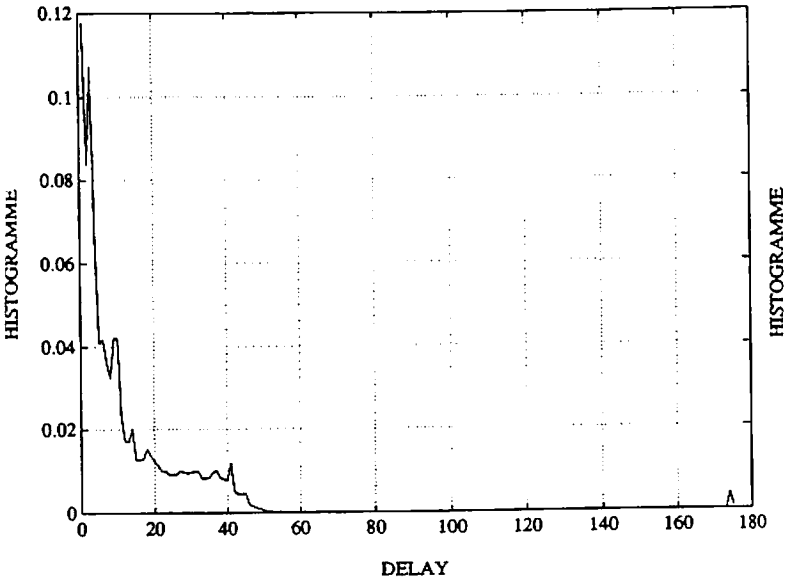

Figure 8: inter-arrival distribution at TxF=20

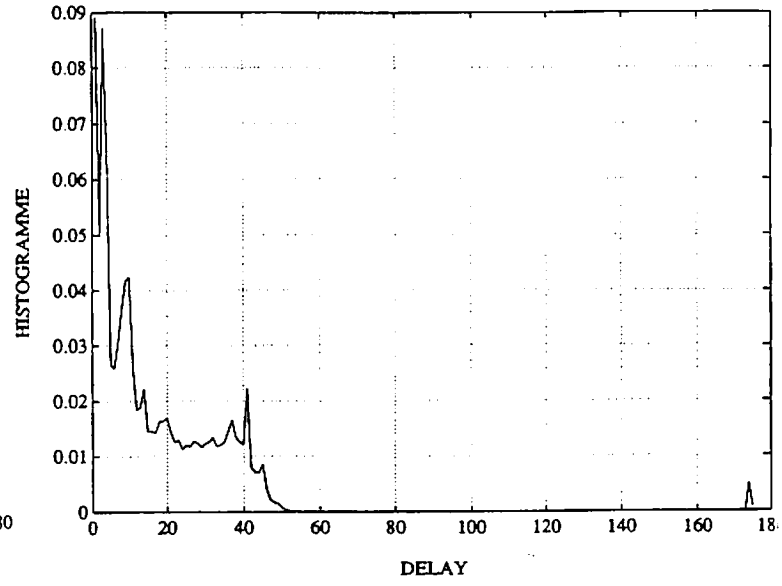

Figure 9: inter-arrival distribution at TxF=30

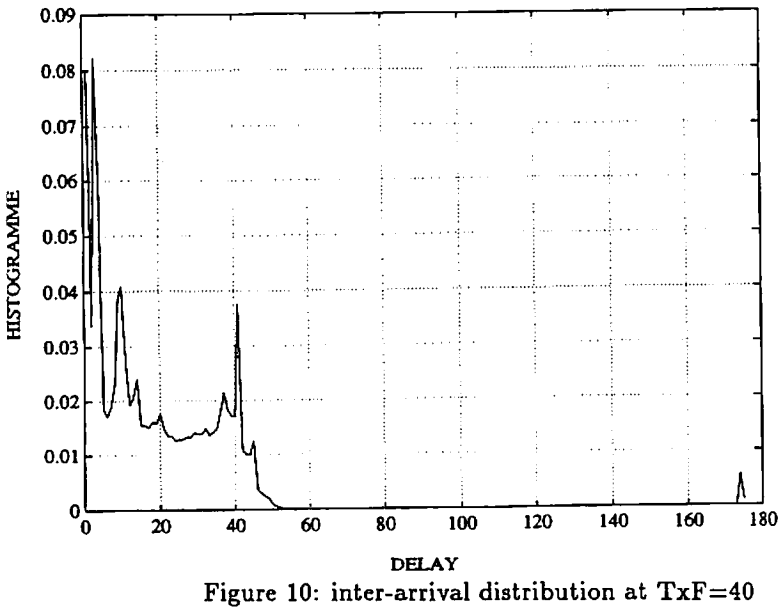

Figure 10: inter-arrival distribution at TxF=40

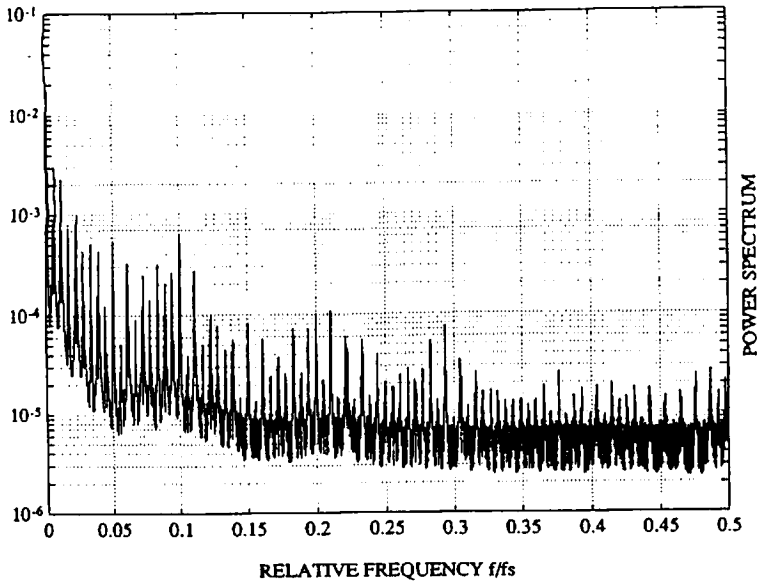

Figure 11: inter-arrival power spectrum at TxF=5

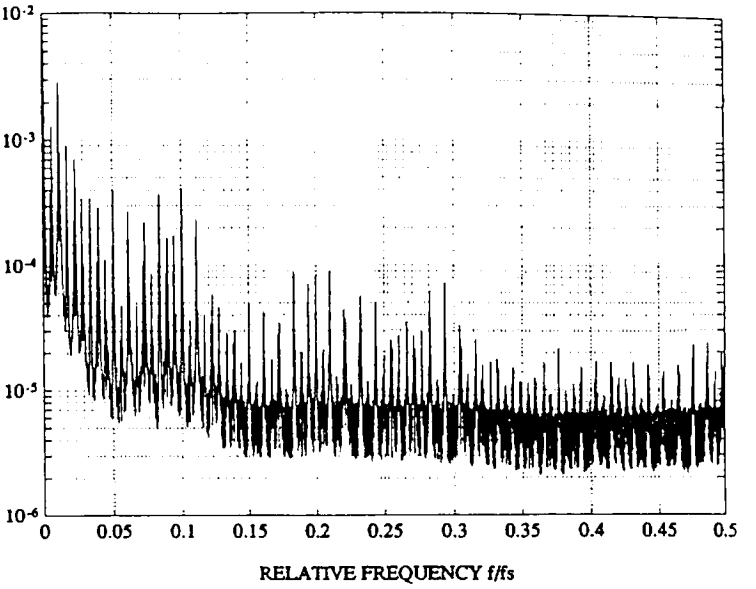

Figure 12: inter-arrival power spectrum at TxF=10

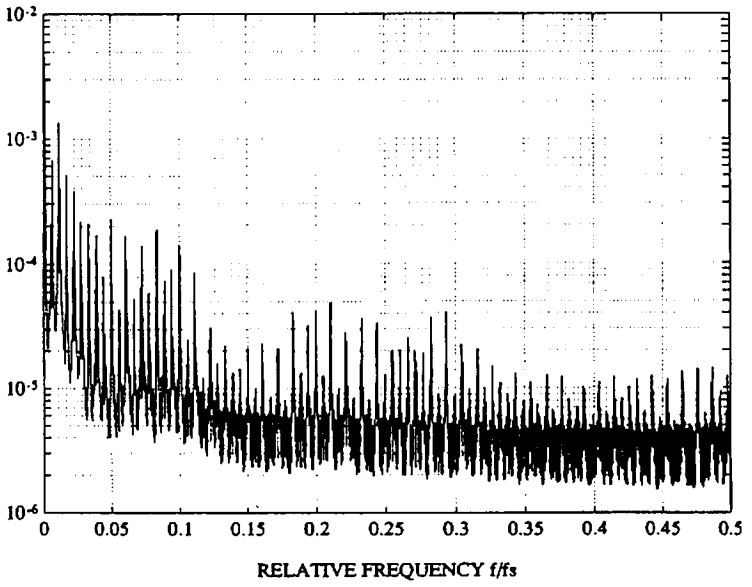

Figure 13: inter-arrival power spectrum at TxF=20

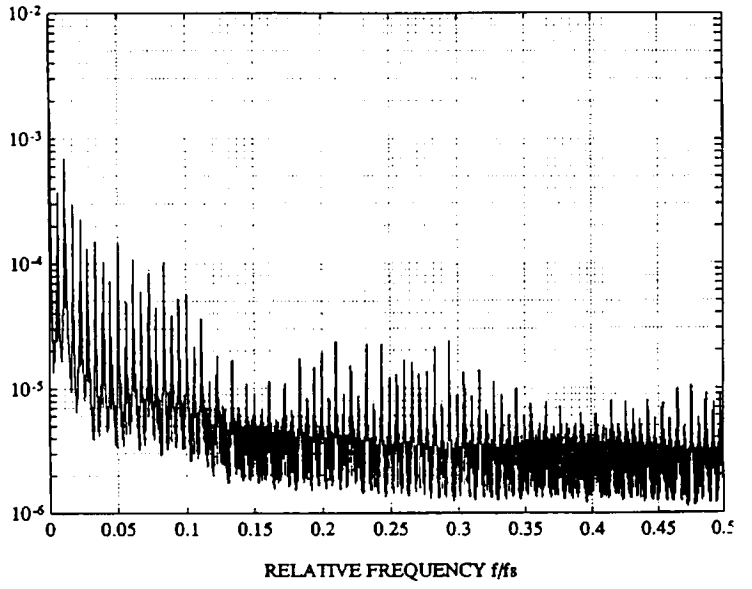

Figure 14: inter-arrival power spectrum at TxF=30

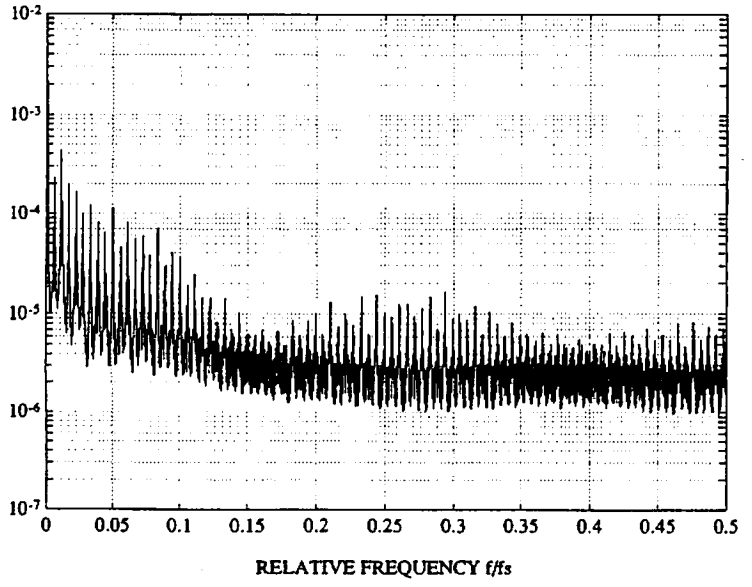

Figure 15: inter-arrival power spectrum at TxF=40

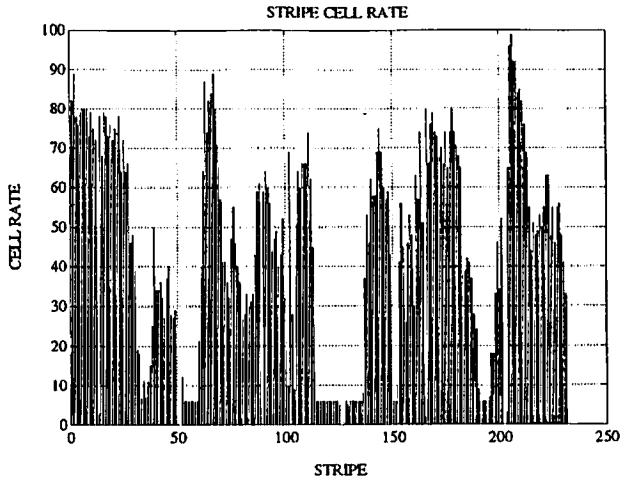

Figure 16: slice cell rates $R_s(n)$ at TxF=5

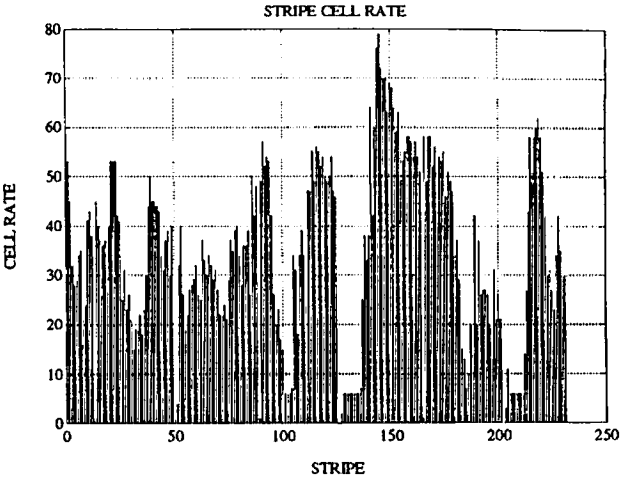

Figure 17: slice cell rates $R_s(n)$ at TxF=10

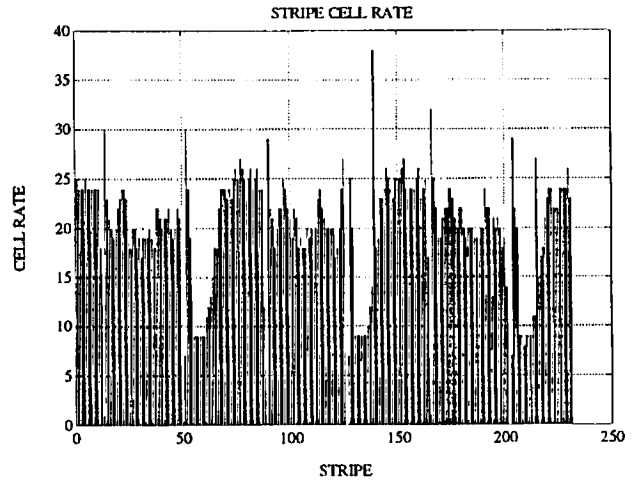

Figure 18: slice cell rates $R_s(n)$ at TxF=20

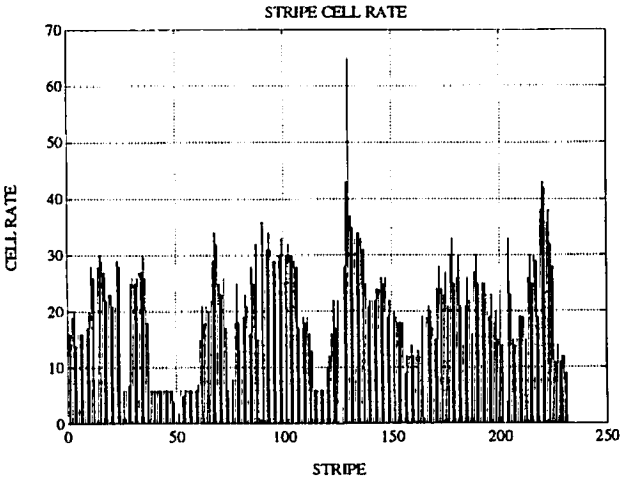

Figure 19: slice cell rates $R_s(n)$ at TxF=30

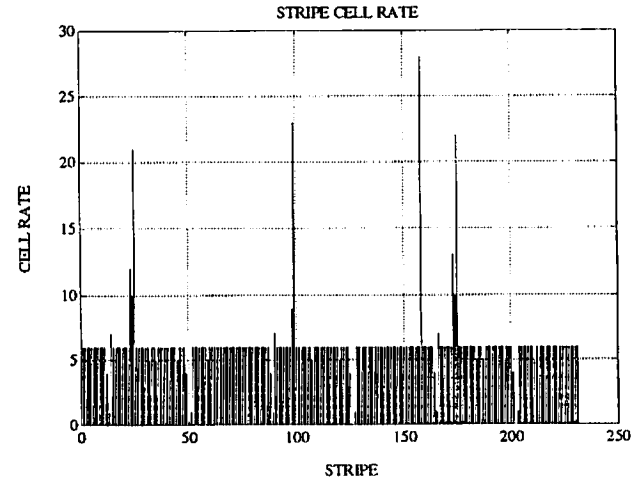

Figure 20: slice cell rates $R_s(n)$ at TxF=40

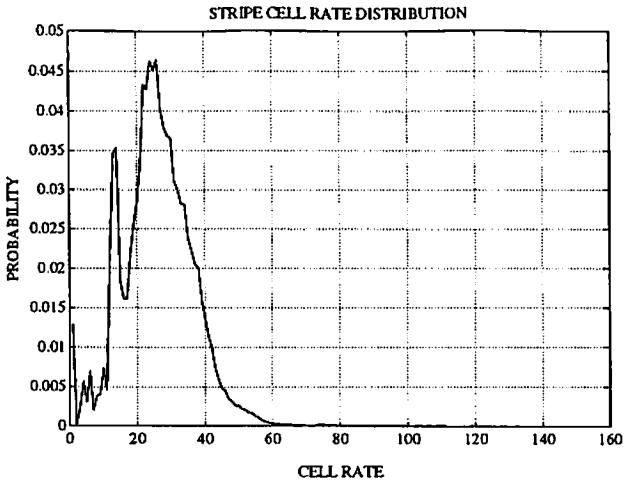

Figure 21: slice cell rate distribution at TxF=5

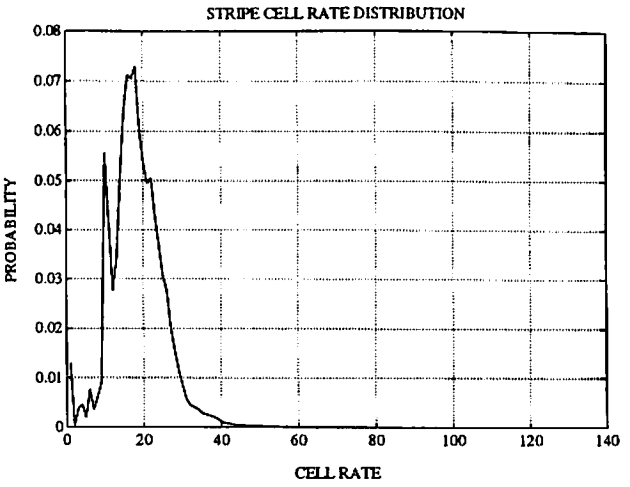

Figure 22: slice cell rate distribution at TxF=10

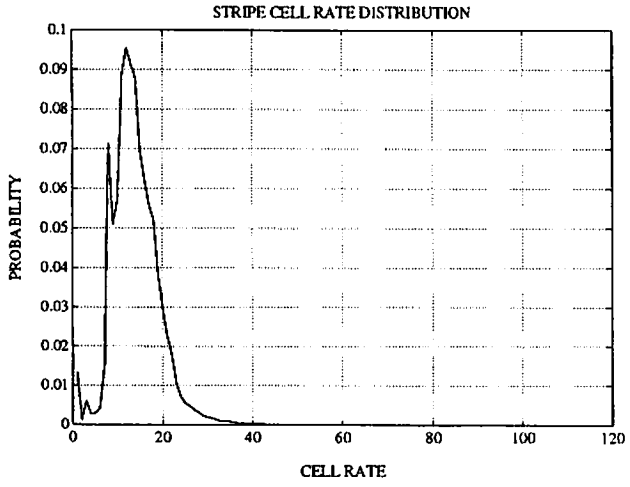

Figure 23: slice cell rate distribution at TxF=20

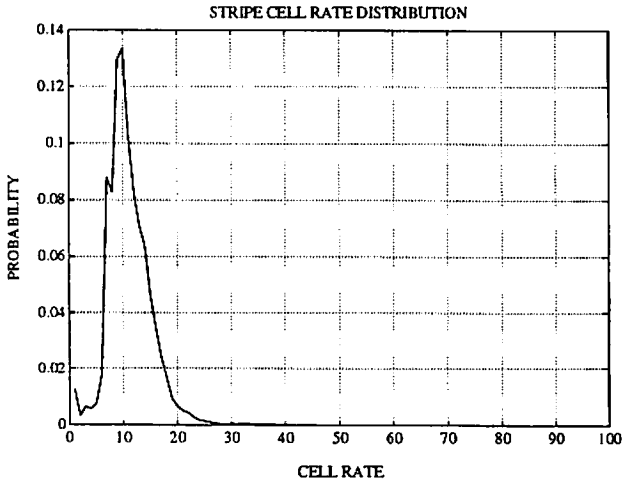

Figure 24: slice cell rate distribution at TxF=30

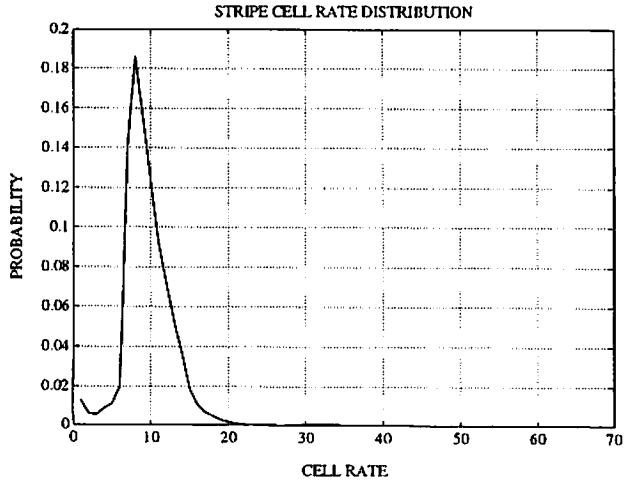

Figure 25: slice cell rate distribution at TxF=40

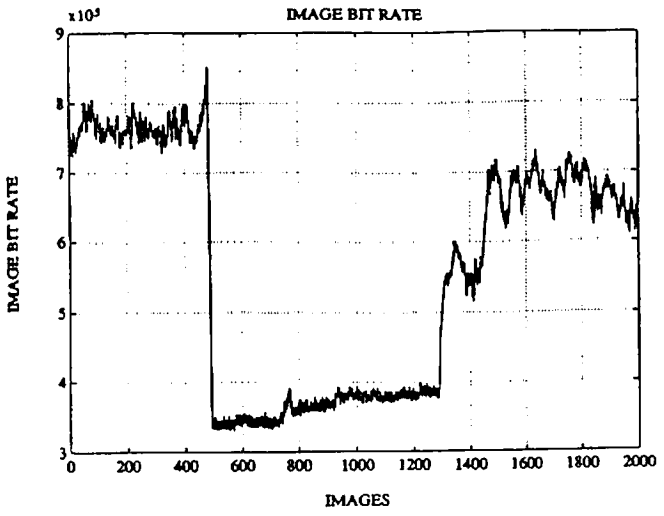

Figure 26: image bit rate graph at TxF=5

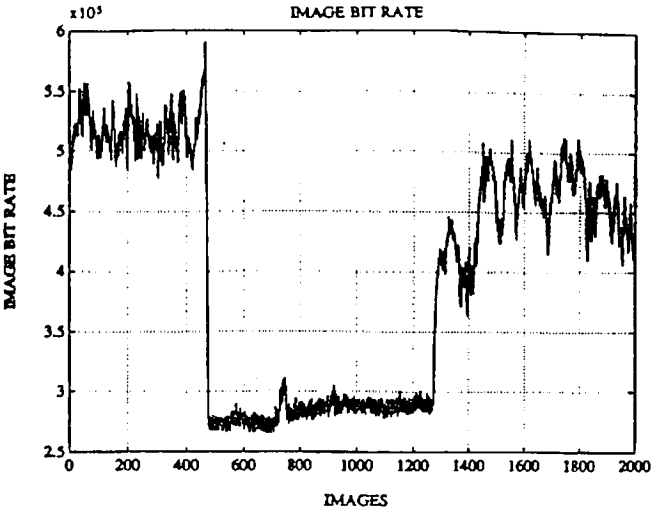

Figure 27: image bit rate graph at TxF=10

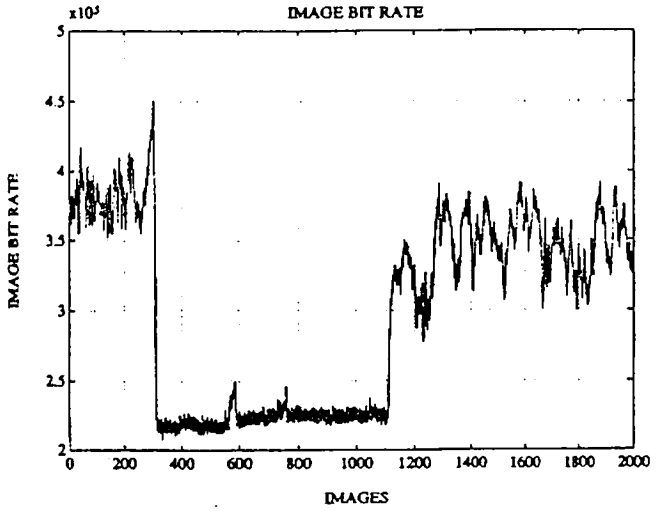

Figure 28: image bit rate graph at TxF=20

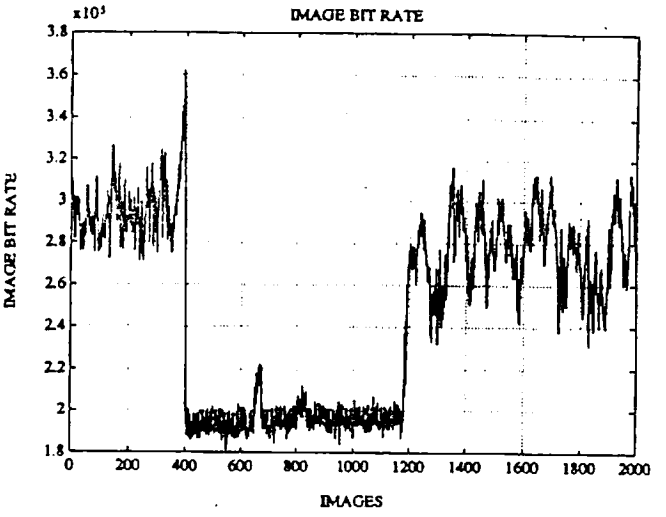

Figure 29: image bit rate graph at TxF=30

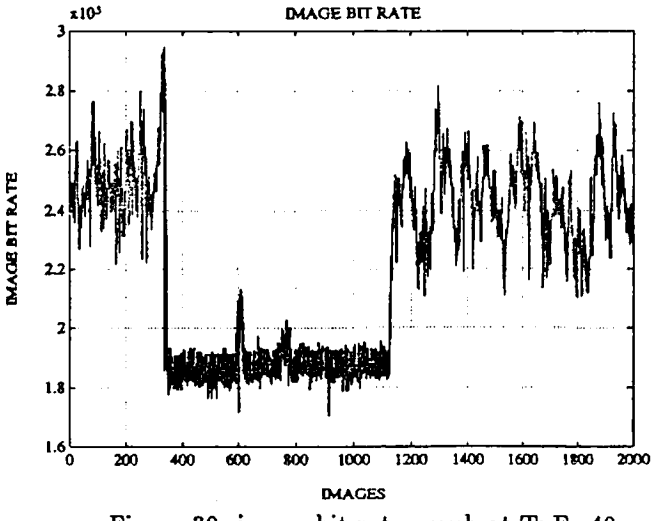

Figure 30: image bit rate graph at TxF=40

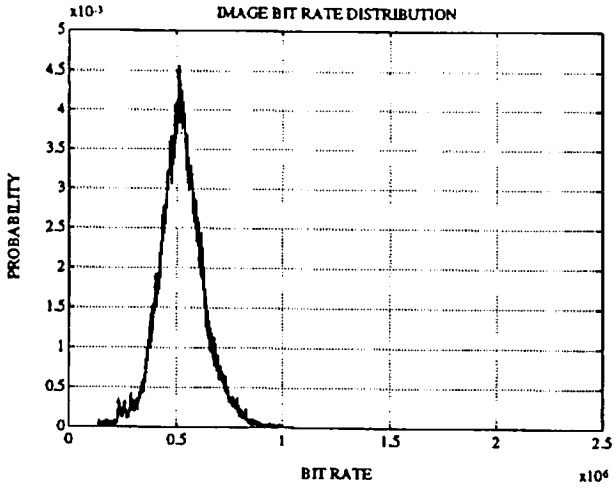

Figure 31: image bit rate distribution at TxF=5

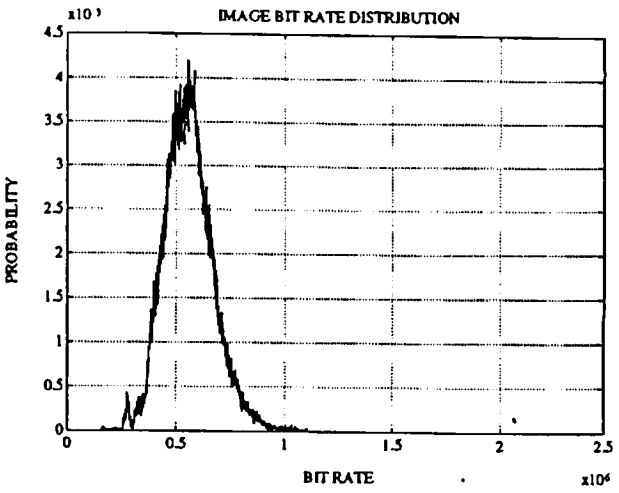

Figure 32: image bit rate distribution at TxF=10

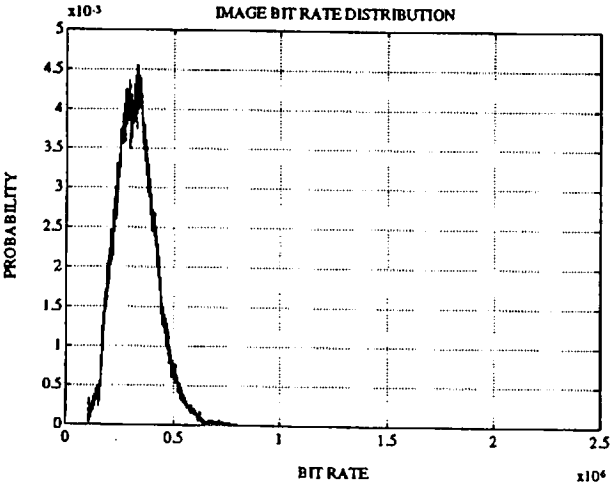

Figure 33: image bit rate distribution at TxF=20

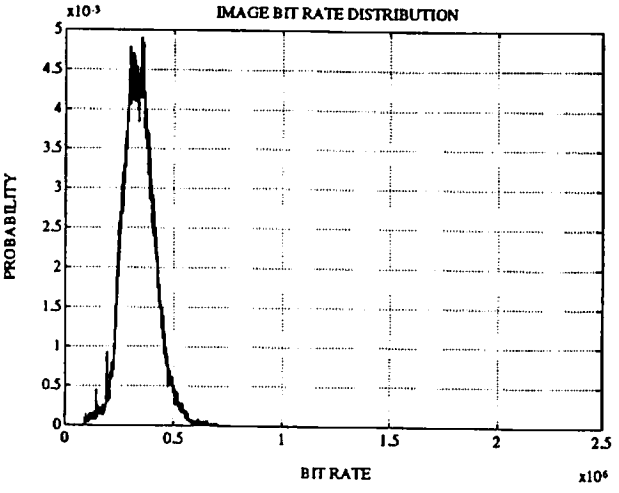

Figure 34: image bit rate distribution at TxF=30

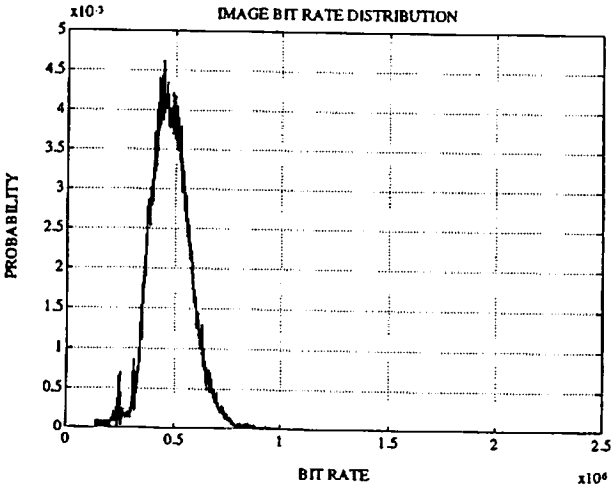

Figure 35: image bit rate distribution at TxF=40